Bicritical universality of the anisotropic Heisenberg model in a crystal field

R. T. S. Freire[1] and J. A. Plascak[2,3,4]

[1]*Universidade Federal de São João del Rei, Campus Dom Bosco, Praça Dom Helvécio, 74-Fábricas 36301-160, São João del Rei, MG-Brazil*

[2]*Departamento de Física, Instituto de Ciências Exatas, Universidade Federal de Minas Gerais, C.P. 702, 30123-970, Belo Horizonte, MG-Brazil*

[3]*Universidade Federal da Paraíba, Centro de Ciências Exatas e da Natureza-Campus I, Departamento de Física-CCEN Cidade Universitária 58051-970, João Pessoa, PB-Brazil*

[4]*Center for Simulational Physics, University of Georgia, Athens, Georgia 30602, USA*

(Received 17 April 2014; revised manuscript received 11 February 2015; published 27 March 2015)

The bicritical properties of the three-dimensional classical anisotropic Heisenberg model in a crystal field are investigated through extensive Monte Carlo simulations on a simple cubic lattice, using Metropolis and Wolff algorithms. Field-mixing and multidimensional histogram techniques were employed in order to compute the probability distribution function of the extensive conjugate variables of interest and, using finite-size scaling analysis, the first-order transition line of the model was precisely located. The fourth-order cumulant of the order parameter was then calculated along this line and the bicritical point located with good precision from the cumulant crossings. The bicritical properties of this point were further investigated through the measurement of the universal probability distribution function of the order parameter. The results lead us to conclude that the studied bicritical point belongs in fact to the three-dimensional Heisenberg universality class.

DOI: 10.1103/PhysRevE.91.032146 PACS number(s): 64.60.Kw, 75.10.−b, 05.10.Ln, 75.40.Mg

I. INTRODUCTION

The three-dimensional classical anisotropic Heisenberg model with competing anisotropies gives rise to multicritical phenomena which have recently raised the interest of many researchers in systems as the XXZ antiferromagnetic model with crystalline anisotropy [1], the Heisenberg model with ferro-antiferromagnetic exchange interactions [2], and exchange ferromagnetic and crystalline anisotropies [2,3]. In particular, it has been recently shown [4] that the multicritical point of the three-dimensional XXZ antiferromagnetic model on a cubic lattice in an external field is, in fact, despite previous debates, a bicritical point whose universality class is the same as the three-dimensional Heisenberg model. On the other hand, Andrade *et al.* [2] have located the bicritical point on the three-dimensional anisotropic Heisenberg model in a crystal field corroborating our previous preliminary location at $(D,T) = [3.95(4),1.73(3)]$ [3], where D is the crystal field in units of the exchange interaction and T is the temperature in units of the ratio of the exchange interaction and the Boltzmann constant. Those authors also claim that this point belongs to the three-dimensional Heisenberg universality class.

In this work we have located the bicritical point of this model with better precision and, in addition, investigated the universal properties of this point, which, to the best of our knowledge, have not been shown in the literature, specially the universal bicritical probability distribution functions (PDFs). Part of this work, concerning the location of the bicritical point, has been recently published elsewhere [5].

The model, simulated on a simple cubic lattice of size L, is defined by the Hamiltonian

$$\mathcal{H} = -J \sum_{\langle i,j \rangle} \vec{S}_i \cdot \vec{S}_j - A \sum_{\langle i,j \rangle} S_i^z S_j^z + D \sum_{i}^{N} \left(S_i^z\right)^2, \quad (1)$$

where $\vec{S}$ stands for a classical three-dimensional spin and $\langle i,j \rangle$ stands for a sum over first-neighbor spins on a lattice of size $N = L^3$ with periodic boundary conditions. The exchange interaction parameter is J, A refers to the easy-axis exchange anisotropy ($A > 0$), and D is related to the easy-plane crystalline interaction ($D > 0$). In this work we used $A = 1$ and, for simplicity, $J = 1$ and $k_B = 1$. The phase diagram of this model is depicted in Fig. 1, as obtained in a previous work [3] for $L = 14$.

The competition between crystalline and exchange anisotropies gives rise to two ordered phases, one where spins tend to align along the z axis (the Ising-like phase) and the other where spins tend to lie on the xy plane (the XY-like phase). These phases are separated by a first-order transition line, whose *terminus* is at a bicritical point, from which two second-order transition lines emerge (the reason for the nomenclature *bicritical*) separating the disordered paramagnetic phase. In order to locate this point, the fourth-order cumulant was calculated along the first-order transition line, which was precisely located through histogram reweighting and analysis of probability distribution functions. The bicritical point was located by the cumulant crossings. Once the bicritical point was located, the universal PDFs for the conjugate extensive variables were obtained and a set of critical exponents were determined. More details about this procedure are given in the subsequent sections.

It is well known that the analysis of probability distribution functions is a very powerful tool to investigate the universality class of statistical physics systems. As the set of critical and/or multicritical exponents, the probability distribution functions are also characteristic of a given specific universality class [6–8]. This strategy was introduced, independently, in 1981 by Binder [6] and Bruce [9] in the study of magnetic systems. Later, in 1992, Wilding and Bruce [10,11], studying the two-dimensional Lennard-Jones fluid, developed further a clever strategy—the field-mixing—which extended the analysis of the probability distribution functions to a variety of statistical mechanics systems [12].

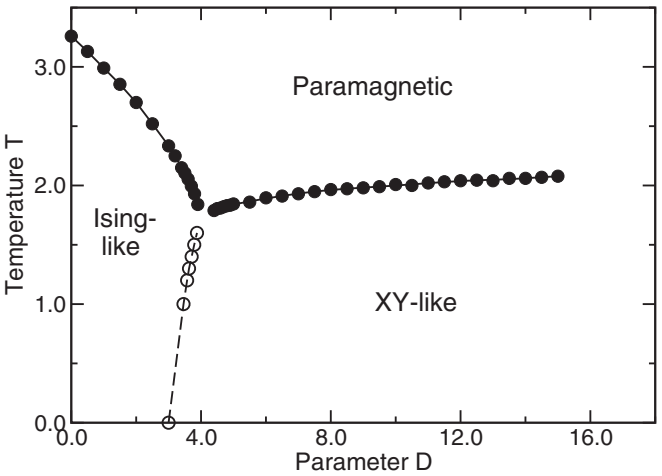

FIG. 1. Phase diagram for the anisotropic Heisenberg model in a crystal field in a cubic lattice ($L = 14$). Lines are only guides to the eyes. The continuous lines indicate second-order phase transitions and the dashed line stands for first-order phase transitions. Error bars are of the size or smaller than symbol sizes.

This technique has since been employed to locate multicritical points and also to determine the universality class of different systems by comparing the PDF of the system with another whose universality class is already known *a priori*, as in the location of the double critical endpoint of the two-dimensional spin-3/2 Blume-Capel model [13] or the tricritical point and double critical endpoint of the vectorial version of the BEG model [14]. On the other hand, when the universality class is not known, this strategy can also be used to locate multicritical points and subsequently characterize the universal multicritical properties, as in the tricritical point of a two-dimensional spin fluid [15]. We, in fact, employed both approaches in this work to investigate bicriticality on the anisotropic Heisenberg model in a crystal field.

Our paper is organized as follows: In Sec. II, we describe the methods of analysis employed in the present work, namely the probability distribution function analysis and the field-mixing technique. In Sec. III, the results are presented along with the finite-size scaling relations employed and, finally, in Sec. IV we present our main conclusions. The Appendix is devoted to discussing the determination of (spurious) critical exponents of this model and its strong dependence on the lattice size.

II. BACKGROUND

A. Universal probability distribution functions

Based on finite-size scaling arguments, analogous to usual finite-size scaling assumptions [6,16], it is expected that, at criticality and large enough system sizes L, the order parameter probability distribution $P(m)$ should obey the following scaling relation [6]:

$$P(m) = bL^{\beta/\nu} P^*(bL^{\beta/\nu} m), \tag{2}$$

where β and ν are the usual critical exponents and m is the order parameter.

Bearing in mind that, near criticality, the singular part f_s of the free energy is a generalized homogeneous function of its parameters [17] and Kadanoff's seminal renormalization group ideas[16,18], one can write for the d-dimensional Ising model

$$f_s(t,m) = L^{-d} f_s(L^{-1/\nu} t, L^{\beta/\nu} m), \tag{3}$$

where $t = (T - T_c)/T_c$.

Considering that the probability distribution function of a finite-size system with dimension L is a function of free energy,

$$P_L(m) \sim \exp[-F(m,T,L)], \tag{4}$$

it is reasonable to assume that the probability function of the order parameter should also obey an analogous scaling relation as described above. Bruce has also demonstrated that the PDF tends to a universal form, based on multispin correlation analysis and renormalization group assumptions [9] and theoretically obtained the universal form for one-, two-, and three-dimensional Ising systems. Binder [6] also obtained the universal PDF for two-, three-, and four-dimensional Ising models.

We use the fourth-order cumulant of the order parameter to locate the bicritical point and subsequently characterize its universality properties by measuring the bicritical universal PDFs of the corresponding extensive thermodynamic variables.

B. Field mixing

Owing to the asymmetry of the first-order transition line (see, e.g., Fig. 1), the employment of field-mixing techniques is necessary. The relevant scaling fields in this case will be linear mixtures of the thermodynamic fields T and D:

$$\eta = \tilde{q} - \tilde{q}_c + r(\tilde{t} - \tilde{t}_c), \tag{5}$$

$$\tau = \tilde{t} - \tilde{t}_c - s(\tilde{q} - \tilde{q}_c), \tag{6}$$

where $\tilde{t} = \beta J$ and $\tilde{q} = \beta D$ and $\tilde{t}_c$ and $\tilde{q}_c$ are the values of these thermodynamic fields at the bicritical point. The parameters r and s are field-mixing parameters that determine the direction of the axes of the relevant scaling fields in the D-T plane. The new extensive variables associated with the scaling fields η and τ are

$$\mathcal{E} = \frac{E - rQ}{1 - rs}, \tag{7}$$

$$\mathcal{Q} = \frac{Q - sE}{1 - rs}, \tag{8}$$

$$\mathcal{M} = M_z, \tag{9}$$

where, considering the model Hamiltonian given by Eq. (1),

$$Q = \frac{1}{L^3} \sum_i^N \left(S_i^z\right)^2, \tag{10}$$

and

$$E = \frac{1}{L^3} \sum_{\langle i,j \rangle} \vec{S}_i \cdot \vec{S}_j. \tag{11}$$

These were the quantities measured during Monte Carlo simulations, along with $C = \frac{1}{L^3} \sum_{\langle i,j \rangle} S_i^z S_j^z$ and the cartesian components of the magnetization per site. These quantities

were stored during each simulation for posterior analysis. The choice of the z component of the magnetization as the order parameter is related to the anisotropic character of the studied model. The magnetization itself is another valid choice for the order parameter and we in fact work with both quantities.

In analogy to the scaling relation obeyed by the order parameter PDF, a similar scaling relation holds for the new extensive variables at criticality:

$$P(\mathcal{Q}) = \frac{1}{1-rs}\lambda_{\mathcal{Q}} L^{y_{\mathcal{Q}}} P^*(\lambda_{\mathcal{Q}} L^{y_{\mathcal{Q}}} \mathcal{Q}), \tag{12}$$

$$P(\mathcal{M}) = \lambda_{\mathcal{M}} L^{\beta/\nu} P^*(\lambda_{\mathcal{M}} L^{\beta/\nu} \mathcal{M}), \tag{13}$$

where β and ν are the usual critical exponents and P^* is a universal, scale-invariant PDF characterizing the bicritical point.

An analogous scaling relation holds for $\mathcal{E}$. For our purposes, though, the variables of interest were $\mathcal{Q}$ and $\mathcal{M}$. Considering that the universal probability distribution functions should be normalized to unit variance, the scale-dependent term $\frac{1}{1-rs}\lambda_{\mathcal{Q}} L^{y_{\mathcal{Q}}}$ can be equated to $1/\sigma$, σ being the standard deviation of $P(\mathcal{Q})$, calculated from Monte Carlo simulations. The same relation holds for $\lambda_{\mathcal{M}} L^{\beta/\nu}$, σ now being the standard deviation of $P(\mathcal{M})$, so that the universal PDF can be obtained by rescaling the PDF extracted from Monte Carlo simulations by the respective standard deviation of the distribution. In this case we get rid of the parameter r and we are left with just s and T in order to recast the PDF into a desired symmetric form. However, the value of r is determined by the slope of the first-order transition line which is already known (for more details see Ref. [7]).

The bicritical scale invariance of the distributions $P(\mathcal{Q})$ and $P(\mathcal{M})$ implies that, at the bicritical point, the fourth-order cumulant should be equal for different system sizes. So, the cumulant was calculated along the first-order transition line so as to locate the cumulant crossing and, consequently, the bicritical point. In order to locate the first-order transition line, we probed $P(\mathcal{Q})$. For a fixed value of the parameter D, and a given lattice size L, we varied the temperature T and the mixing parameter s within the histogram reweighting scheme so as to symmetrize the PDF for $\mathcal{Q}$ and locate the first-order transition line.

In this work, we also investigated the fourth-order cumulant of the total magnetization and of its z component. The fourth-order cumulant of the magnetization is defined, in principle, as

$$U = 1 - \frac{\langle (m - \langle m \rangle)^4 \rangle}{3\langle (m - \langle m \rangle)^2 \rangle^2}. \tag{14}$$

At the bicritical point, however, $\langle m_z \rangle = \langle m \rangle = 0$, so that the fourth-order cumulant is written

$$U = 1 - \frac{\langle m^4 \rangle}{3\langle m^2 \rangle^2}. \tag{15}$$

An analogous equation holds for the z component of the magnetization.

III. RESULTS

Monte Carlo simulations were performed combining one Metropolis [19] sweep and four Wolff [20] steps in a hybrid scheme [21] in order to reduce the effects of critical slowing down. The Wolff algorithm was adapted to take into account the anisotropies of the model, according to the prescription described by Ala-Nissila [22] and also the dimensionality of the lattice. A simple cubic lattice with periodic boundary conditions was used with system sizes $L = 16, 18, 20, 22, 24, 30, 34, 40, 44$, and very long runs were performed, ranging from 280 million to 1.5 billion hybrid Monte Carlo steps (HMCS) so as to achieve good precision, specially on the calculation of cumulants. We also extended the analysis for $L = 60, 64$, and 70 for reasons that will be clear below. We used $100L^2$ HMCS for thermalization.

Owing to the asymmetry of the first-order transition line, the field mixing technique was employed along with the multidimensional histogram method [23–26] so that we could probe the probability distribution of the extensive conjugate variable $\mathcal{Q}$ and precisely locate the first-order transition line. As we are investigating a first-order phase transition, the occurrence of two symmetric wells in the free-energy landscape corresponds to a double-peak probability distribution function of the conjugate extensive variable $\mathcal{Q}$. Therefore, in order to precisely locate the first-order transition line, the symmetrization of the probability distribution function was performed for several values of the parameter D and each lattice size L. This was (initially) done varying the field-mixing parameter s and the temperature T, obtaining the PDF for the variable $\mathcal{Q}$ and evaluating visually the symmetrization. This has been, however, a tedious and time-consuming task.

In order to improve precision and efficiency, we developed a Fortran computational routine. The aim of this automatization was to (1) locate both peaks of the first-order probability distribution function, (2) minimize the difference between heights of these peaks and, once the peaks were equalized, (3) minimize the difference in area under both peaks. From our study we observed that the difference in height of the peaks as a function of temperature for a given value of s is a smooth, well-behaved function, with a single minimum, so that we could write a computational routine to locate this minimum up to a very good precision. In other words, the peak height difference could be minimized down to a very low tolerance (of the order of 10^{-10}). This process was triggered with an initial guess to the location of the minimum in temperature and an initial temperature step ΔT, for a definite value of the parameter s. Once the probability distribution is constructed for the initial temperature, the temperature is incremented by ΔT and the probability distribution is again obtained for this new temperature. Histogram reweighting is employed to obtain this distribution within the temperature range. A subroutine is used to precisely locate the peaks of the distribution (essentially comparing the probability intensity for each abscissa value on the probability distribution) along with the peak height difference. The variation of this peak difference for the used ΔT is then calculated and, if this variation is positive, the sign of ΔT is reversed in order to guarantee that the routine is consistently heading toward the single minimum of the peak height difference versus temperature curve. The routine also keeps track of the product of the inclination of this curve for two subsequent temperature steps so that when the minimum is surpassed the change in sign of this product is followed by a sign reversal in ΔT,

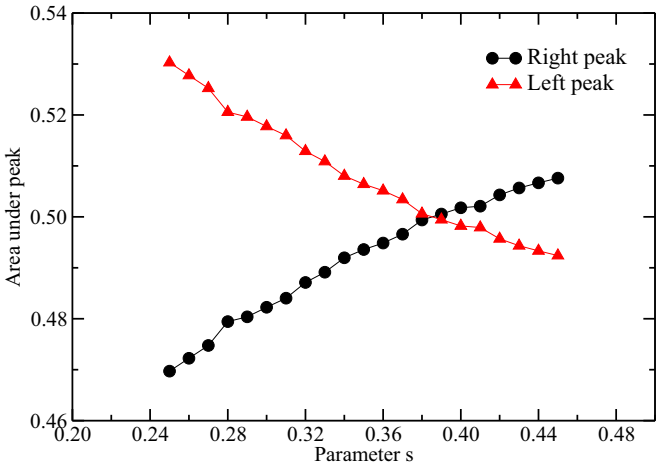

FIG. 2. (Color online) Area under each of the peaks as a function of the parameter s ($L = 20$). This plot is obtained once the peak heights are equalized, so that the symmetrization of the probability distribution is related to value of s where the area for both peaks coincide.

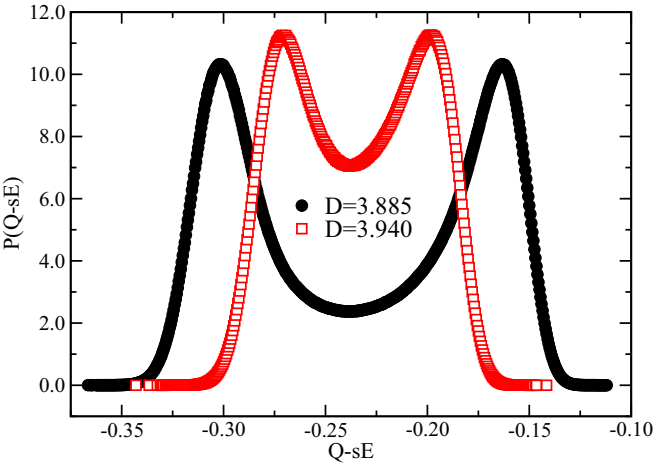

FIG. 3. (Color online) Probability distribution function for the field-mixing extensive conjugate variable $Q - sE$ ($L = 20$). The distributions displayed refer to two different points along the first-order line. Error bars are of the size or smaller than symbol sizes. Distributions normalized to unit norm.

which is also rescaled to half its value. This step ensures that the algorithm progressively approaches the minimum and the overall procedure is repeated until the peak height difference falls into the desired tolerance. This process is performed for a range of values of the parameter s.

Once the peak height difference was minimized, the difference in area under both peaks as a function of s should also be minimized so as to obtain the values of s and T for symmetrization. The routine also measures, after the peaks are equalized in height, the area under each peak, and although it is also possible to visually identify a single minimum, the area difference curve as a function of s, calculated through the trapezoidal rule, displays noise (despite our efforts to suppress it) to an extent that the computational routine could be trapped in shallow, spurious troughs, precluding the location of the real minimum. Therefore, the area symmetrization was performed visually, plotting the area under the right and left peaks as a function of the parameter s (see Fig. 2 for a clear illustration). A similar plot was obtained as a function of T so as to determine the temperature value for symmetrization. The probability curves displayed in Fig. 3 were obtained through this method.

Having obtained, for a given value of the parameter D, the pseudotransition temperature for each lattice size, we determined the transition temperature through finite-size scaling analysis. Repeating this process for several values of D, we finally obtained the first-order transition line. In Fig. 4, the finite-size scaling analysis is shown for two different values of the parameter D along the first-order line. We have noted that for this part of the work the smaller lattice sizes were enough to locate the transition line. However, as will be seen below, larger lattices and quite longer simulations needed to be taken in order to get the multicritical point.

The cumulant, defined in Eq. (15), was calculated at the transition temperature for each lattice size. At the bicritical point, the fourth-order cumulant should coincide for sufficiently large system sizes. Using this crucial fact, we were able to locate the bicritical point. All points in the cumulant curves for all lattice sizes were initially calculated with no extrapolation through the histogram method (Figs. 5 and 6). Histogram reweighting was then performed in the vicinity of the crossing point initially obtained for better precision. The cumulant crossing for the magnetization reveals a bicritical point located at $D_{bc} = 4.0022(6)$, which corresponds to a bicritical temperature $T_{bc} = 1.7365(6)$ (Fig. 7). On the other hand, the analysis of the fourth-order cumulant of the z component of the magnetization (Fig. 8) yields $D_{bc} = 4.0099(9)$ and $T_{bc} = 1.7448(9)$. It is worth noting, however, that despite this discrepancy, as the lattice size increases, the cumulant crossing for the magnetization (z component of the magnetization) tends to occur at slightly higher (lower) temperatures (compare Figs. 7 and 8). This behavior suggests that this discrepancy should fade away for large enough lattice sizes. Taking both locations into account yields a mean value of $D_{bc} = 4.006(5)$ and $T_{bc} = 1.741(5)$.

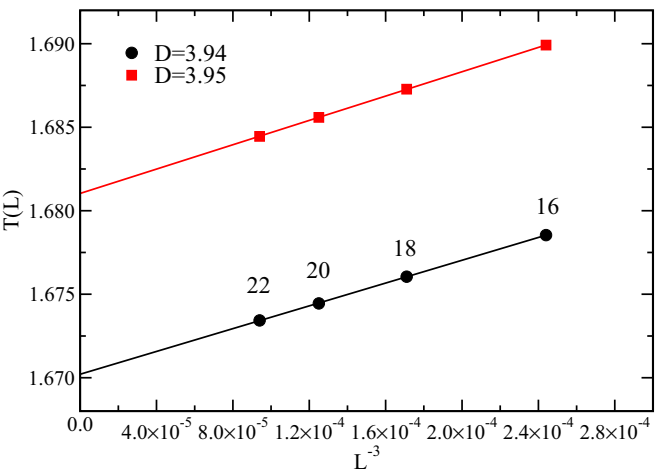

FIG. 4. (Color online) Finite-size scaling analysis for two different points along the first-order line. The line is the best fit to the data points. Error bars are smaller than symbol sizes.

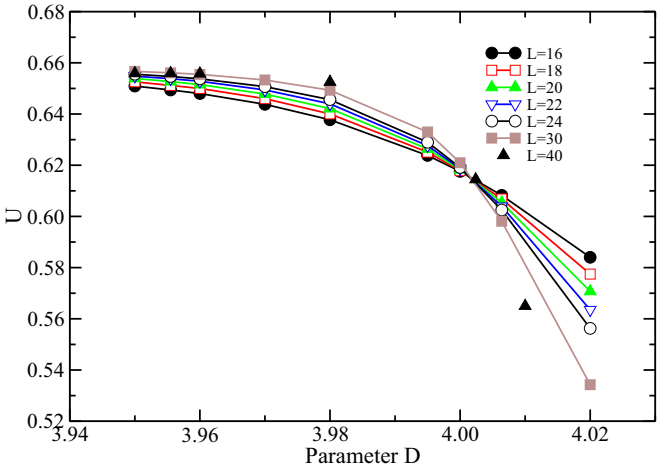

FIG. 5. (Color online) Fourth-order magnetization cumulant for the three-dimensional anisotropic Heisenberg model in a crystal field. Lines are only guides to the eyes. Error bars are of the size or smaller than symbol sizes.

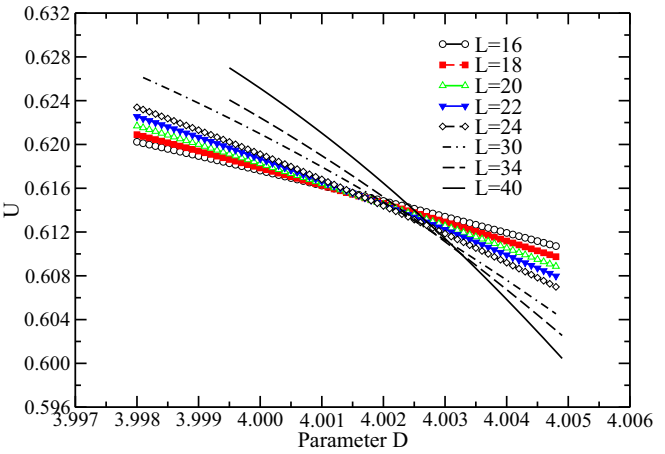

FIG. 7. (Color online) Fourth-order magnetization cumulant for the three-dimensional anisotropic Heisenberg model in a crystal field. Data obtained through histogram reweighting from a simulation in the vicinity of the bicritical point.

In Fig. 9, the first-order transition line is depicted, along with its *terminus* at the bicritical point. We were not able to probe its subsequent analytical extension owing to the fact that at such high values of D in the vicinity of the bicritical point, the two symmetric wells in the free-energy landscape were already too shallow for the lattice sizes used. Therefore, the double-peaked probability distribution function for the field mixing extensive conjugate variable $Q - sE$ were not observed so that the symmetrization process previously described could not be performed. The first-order transition temperature for $3.98 \leqslant D \leqslant 4.02$ were obtained using the regression line $T(D)$ computed from the points along the first-order line obtained for $D \leqslant 3.97$. On the other hand, the cumulant crossing itself reveals that such an extrapolation was good enough for the range used, since the unique point

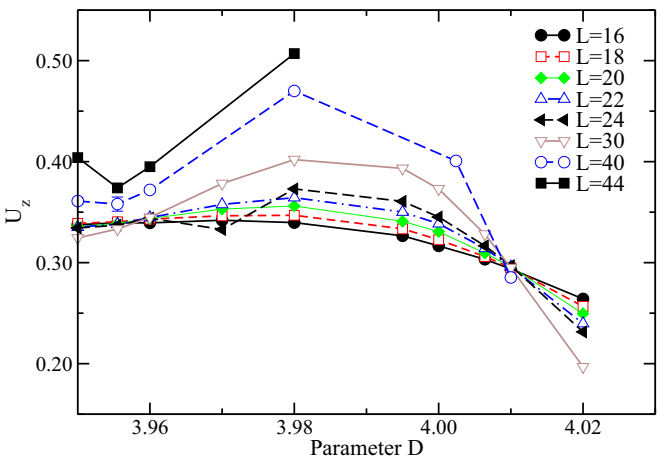

FIG. 6. (Color online) Fourth-order cumulant for the z component of the magnetization for the three-dimensional anisotropic Heisenberg model in a crystal field. Lines are only guides to the eyes. Error bars not shown are of the size or smaller than symbol sizes. Only some points are depicted for $L = 40$ and $L = 44$ in order to show that the crossing at the vicinity of $D = 3.9555$ is in fact spurious.

where the cumulants for different lattice sizes cross could be achieved from this extrapolation with good precision.

It is important to note, however, that the updated location of the bicritical point presented here is apart from the one reported in a previous work [5] [$D_{bc} = 3.9555(4)$ and $T_{bc} = 1.6868(4)$]. The extended and more thorough investigation of the fourth-order cumulant along with the bicritical universal probability distributions lead us to conclude that the bicritical point location is in fact ahead, as previously presented. This behavior was revealed, however, only extending the analysis up to larger lattice sizes. As shown in Fig. 6, the cumulant crossing in the vicinity of $D = 3.9555$ is in fact spurious, and does not occur for $L \gtrsim 40$. The fourth-order cumulant of the magnetization has revealed itself a much more well-behaved quantity in comparison to the its z component counterpart, which also demanded more extensive simulations and very long runs for better accuracy.

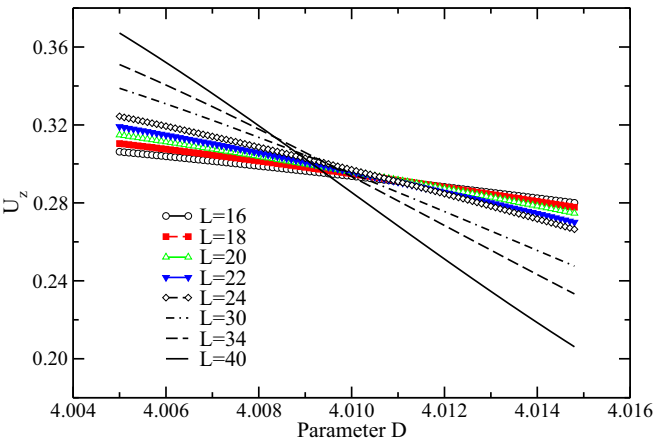

FIG. 8. (Color online) Fourth-order cumulant for the z component of the magnetization for the three-dimensional anisotropic Heisenberg model in a crystal field. Data obtained through histogram reweighting from a simulation in the vicinity of the bicritical point.

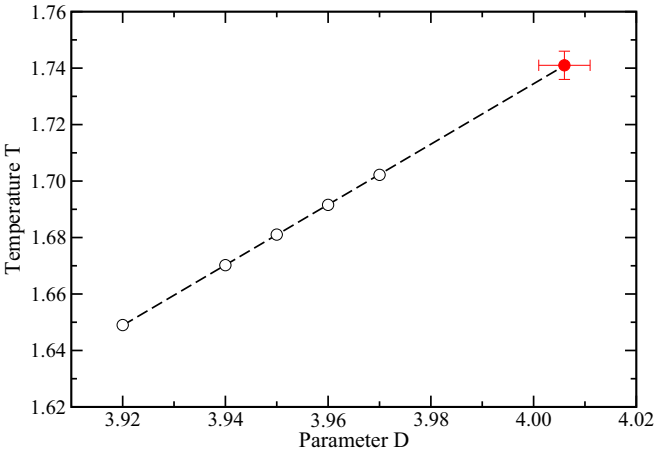

FIG. 9. (Color online) First-order transition line on the D-T plane, obtained through the procedure described in the text. The bicritical point is represented by a full circle with error bars. The line is the best fit to the data. Error bars when not shown are smaller than symbol sizes.

In order to characterize the universality class of the bicritical point, the universal PDF of the magnetization was obtained for each lattice size. As expected, the universal PDFs reasonably coincide for sufficiently large system sizes (Fig. 10). Histogram reweighting was used to screen the universal PDFs within the error bars in order to achieve the best collapse. All PDFs are normalized to unit norm and variance. It is noteworthy that, for the lattice sizes used, namely $L \leqslant 40$, the universal PDF for the order parameter analyzed is similar but does not match the respective universal PDF, which characterizes the three-dimensional Heisenberg model (shown on Fig. 10 for comparison). The universal PDF for the Heisenberg model was obtained for $L = 40$, averaging over one billion HMCS. In addition, if one desires to compute the bicritical exponents from these lattice sizes one achieves a

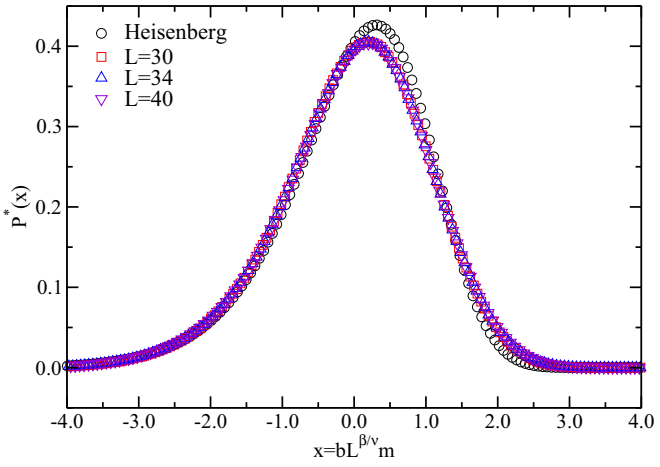

FIG. 10. (Color online) Bicritical universal probability distribution function for the magnetization ($L \leqslant 40$). The distribution is scaled to unit norm and variance. Lines are only guides to the eyes. Error bars are smaller than symbol sizes. Note the discrepancy with the universal PDF for the three-dimensional Heisenberg model. Compare this graph with Fig. 11.

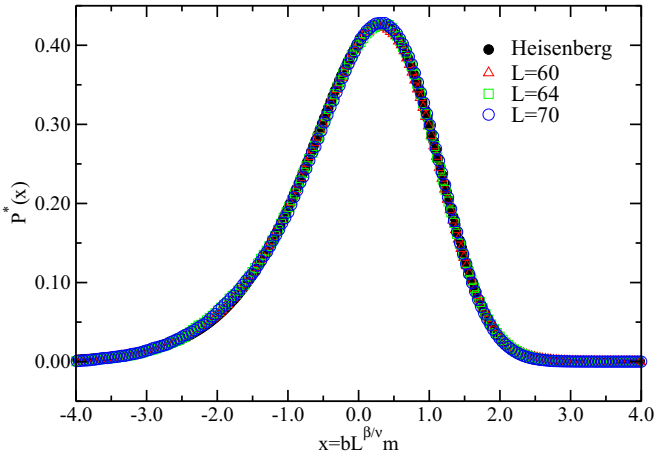

FIG. 11. (Color online) Bicritical universal probability distribution function for the magnetization ($L \geqslant 60$). The distribution is scaled to unit norm and variance. Error bars are smaller than symbol sizes. Observe, for system sizes large enough, the collapse with the universal PDF for the three-dimensional Heisenberg model. Compare this graph with Fig. 10.

spurious result. Some details of what happens in this case are given in the Appendix.

Owing to the similarity of the distribution functions depicted in Fig. 10 and the universal Heisenberg distribution, we extended the PDF analysis to even larger system sizes, namely, $L = 60$, 64, and 70. Considering limited computing time, simulations ranging from 180 million to 234 million HMCS were now performed. The smoothness of the PDFs obtained with small error bars suggests, however, that such statistics were already satisfactory. Using histogram reweighting, we were able indeed to show that the probability distribution function of the anisotropic Heisenberg model reasonably matches the PDF of the three-dimensional Heisenberg model, thus revealing that the model studied belongs to the Heisenberg universality class (Fig. 11). The collapse occurs, for all lattice sizes, at

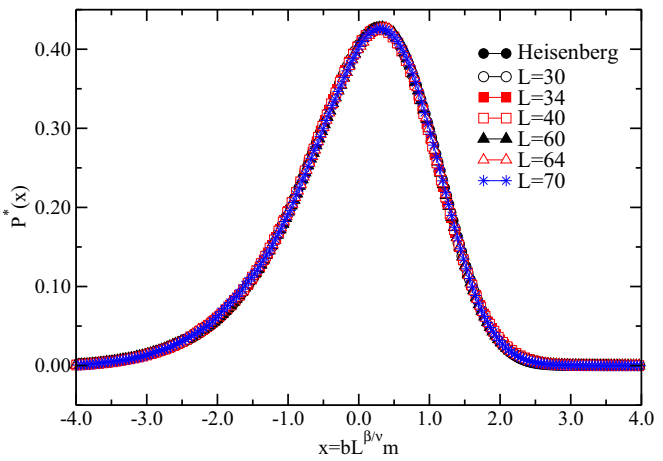

FIG. 12. (Color online) Individual collapse of the PDF for a given lattice size over the universal PDF for the three-dimensional Heisenberg model. The collapse for each lattice size occurs at a different value of T and D. Lines are only guides to the eyes.

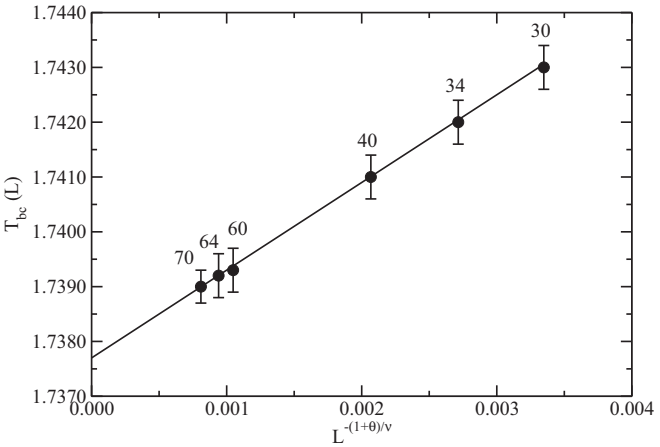

FIG. 13. Finite-size scaling analysis for the bicritical temperature. The line is the best fit to the data.

$D = 4.0036$ and $T = 1.7392$, which agrees, within error bars with our previous result, at $(D_{bc}, T_{bc}) = [4.006(5), 1.741(5)]$.

In order to verify our results, we employed yet another method to locate the bicritical point. Considering that the universality class of the model in study is known *a priori*, we sought the collapse of the PDF for a given lattice size over the universal PDF of the Heisenberg model, tuning the parameters D and T and generating the probability distribution using the multidimensional histogram method (Fig. 12).

The bicritical temperature was thus determined through finite-size scaling analysis of the temperatures $T_{bc}(L)$ obtained above:

$$T_{bc}(L) = T_{bc} + aL^{-(1+\theta)/\nu}, \tag{16}$$

being $\theta = 0.179$ the correction to scaling exponent and $\nu = 0.7036$, the expected value for the three-dimensional Heisenberg model [27]. The value of θ was the one that minimized χ^2 on the regression of the linearized function above. From the analysis (Fig. 13), we obtained $T_{bc} = 1.7377(1)$, which corresponds to $D_{bc} = 4.0033(1)$ on the first-order transition line previously located. This value also agrees with our previous result obtained from the crossing of cumulants. This method proved to be in fact more efficient, since the collapse of the probability distribution function of a given lattice size over the PDF of the Heisenberg model is enough to prove that both models belong to the same universality class, while the crossing of the cumulants demanded larger lattice sizes. Considering the wide range of lattice sizes used and the good quality of the regression analysis, we take this result as the best estimate we have obtained for the location of the bicritical point. In addition, it becomes clear from the small value of the correction to scaling exponent $\theta = 0.179$ the need to extend the analysis to lattice sizes large enough in order to achieve the real finite-size scaling behavior (which is discussed in more detail in the Appendix).

IV. CONCLUSIONS

In summary, we have thoroughly investigated the bicritical properties of the anisotropic Heisenberg model in a crystal field on a simple cubic lattice for $A = 1$. The bicritical point was located with better precision at $D = 4.0033(1)$ and $T = 1.7377(1)$. The universal probability distribution function of the order parameter was obtained, leading us to conclude that the bicritical point belongs to the three-dimensional Heisenberg universality class. Since the Ising- and XY-like phases must be equal at the bicritical point, the xy magnetization vector turns equal to the z magnetization vector, which is accomplished only when the magnetization is zero. Thus, the model regains in a certain way its isotropic character at the bicritical point and therefore it is reasonable to expect that the bicritical point should belong to the isotropic three-dimensional Heisenberg universality class. It is interesting to note that the presence of symmetry-breaking fields may change the universality class [23], but such effect does not occur in the anisotropic Heisenberg model studied.

ACKNOWLEDGMENTS

R.T.S.F. is indebted to Dr. D. P. Landau for fruitful discussions and Dr. G. Weber for generous allocation of CPU time and disk space at the Statistical Physics Simulation Laboratory, Universidade Federal de Minas Gerais. We acknowledge financial support from the Brazilian agencies CNPq (Grant No. 402091/2012-4), CAPES, and FAPEMIG.

APPENDIX

It is worth noting that the size of the system studied was in fact crucial for the determination of the universality class of the model when we used the crossing of the fourth-order cumulant. As shown in Fig. 10, finite-size effects are still manifest for systems as large as $L = 40$ so that the universal probability function of the anisotropic model does not match the universal PDF for the Heisenberg three-dimensional model, which would lead to the incorrect conclusion that the anisotropic model belongs to a distinct universality class. One could think (as we did) of determining the bicritical exponents so as to investigate this assertion. This approach, however, poses the same problem, as shown below, as we determine critical exponents at $D_{bc} = 4.006(5)$ and $T_{bc} = 1.741(5)$, the location of the bicritical point obtained from the crossing of cumulants for $L \leqslant 40$.

The normalization of the universal probability distribution (in order to obtain unit variance) yields a scaling relation for the standard deviation $\sigma = \sqrt{\langle m^2 \rangle}$ (considering $\langle m \rangle = 0$ at criticality) as function of system size:

$$\sigma = \frac{1}{b} L^{-\beta/\nu}, \tag{A1}$$

through which $\beta/\nu = 0.65(1)$ was obtained (see finite-size scaling analysis in Fig. 14). This ratio was also obtained from the scaling analysis of the magnetization,

$$\langle m \rangle \sim L^{-\beta/\nu}, \tag{A2}$$

from which $\beta/\nu = 0.66(1)$ (Fig. 15). Both values agree within error bars and yield an average of $\beta/\nu = 0.66(2)$.

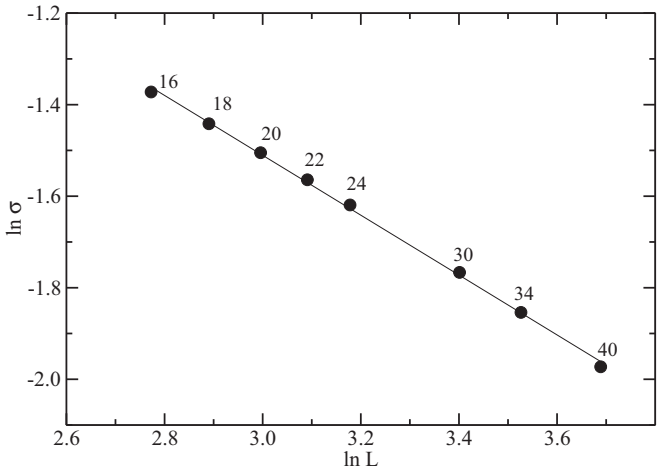

FIG. 14. Finite-size scaling analysis of the standard deviation of the magnetization PDF at the bicritical point. The line is the best fit to the data. Error bars are smaller than symbol sizes.

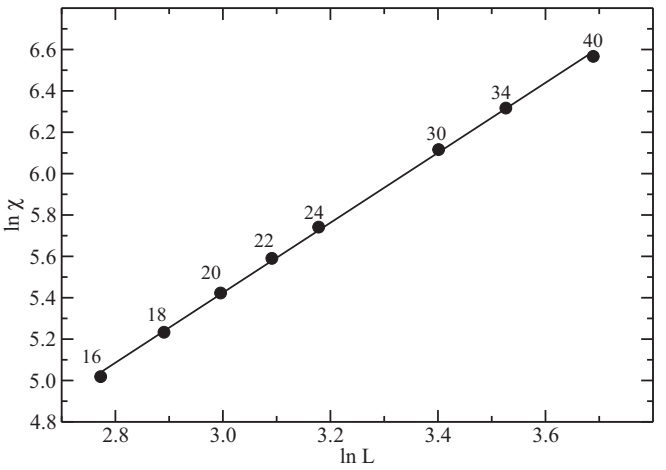

FIG. 16. Finite-size scaling analysis for the true ($\langle m\rangle = 0$) magnetic susceptibility at the bicritical point. The line is the best fit to the data. Error bars are smaller than symbol sizes.

The maximum of the true (considering $\langle m\rangle = 0$ at criticality) magnetic susceptibility,

$$\chi = \frac{L^3}{T}(\langle m^2\rangle), \tag{A3}$$

scales as

$$\chi \sim L^{\gamma/\nu} \tag{A4}$$

at the bicritical point, from which we obtained $\gamma/\nu = 1.69(2)$ (Fig. 16).

The value of the exponent ν was obtained through finite-size scaling analysis of the logarithmic derivative of $\langle m\rangle$ and $\langle m^2\rangle$, whose scaling behavior is given by [23]

$$\frac{\partial}{\partial K}\ln\langle m^n\rangle = aL^{-1/\nu}, \tag{A5}$$

at criticality, where

$$\frac{\partial}{\partial K}\ln\langle m^n\rangle = \frac{\langle m^n E\rangle}{\langle m^n\rangle} - \langle E\rangle. \tag{A6}$$

This analysis yields $\nu = 0.74(2)$ for the logarithmic derivative of $\langle m\rangle$ and $\nu = 0.73(2)$ from $\langle m^2\rangle$, which agree within error bars and yield a mean value $\nu = 0.74(2)$; see Fig. 17. Considering this result, the bicritical exponents obtained were $\beta = 0.49(3)$ and $\gamma = 1.25(5)$.

It is worth noting that the bicritical exponent ratios obtained even obey the scaling relation $d = 2\beta/\nu + \gamma/\nu = 3.01(6)$, d being the spatial dimensionality of the lattice, which, along with the good quality of the regression analysis, corroborates our determination of critical exponents.

The values of the bicritical exponents therefore lead us to (erroneously) conclude that the bicritical point of the

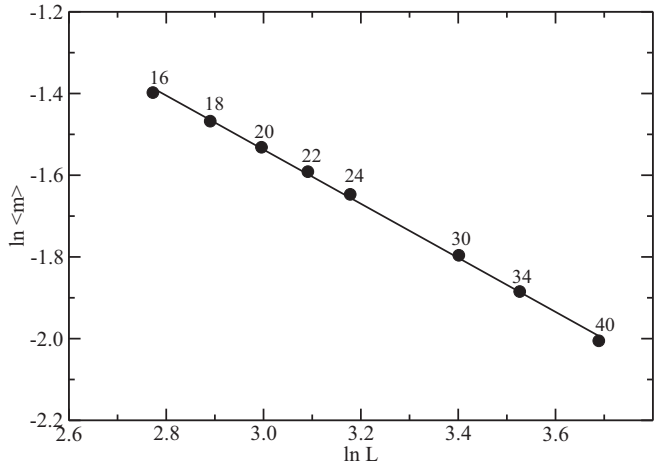

FIG. 15. Finite-size scaling analysis for the magnetization at the bicritical point. The line is the best fit to the data. Error bars are smaller than symbol sizes.

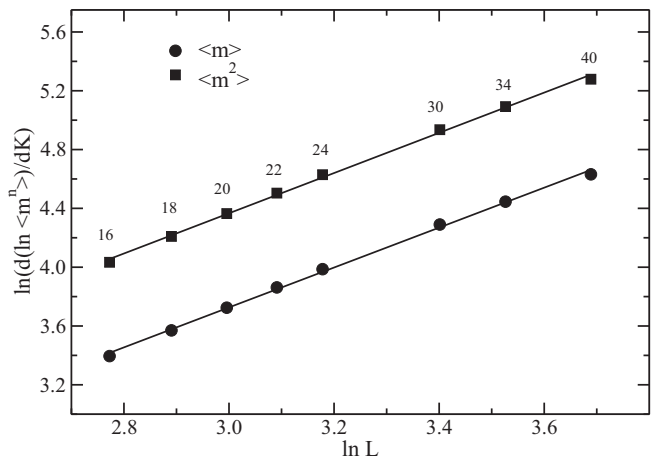

FIG. 17. Finite-size scaling analysis for the logarithmic derivative of $\langle m\rangle$ and $\langle m^2\rangle$. The line is the best fit to the data. Error bars are smaller than symbol sizes.

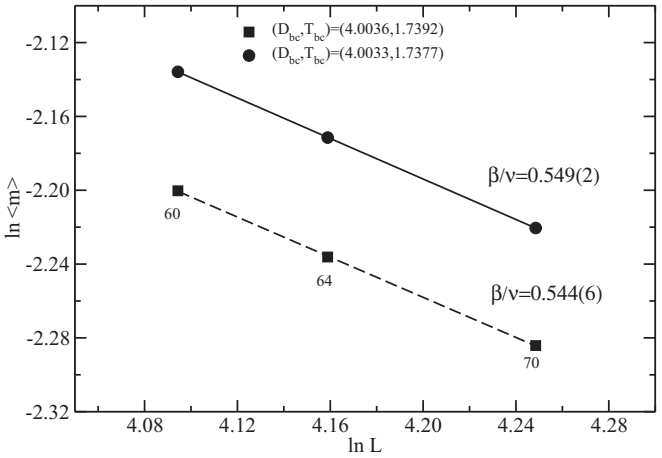

FIG. 18. Finite-size scaling analysis for the magnetization at the bicritical point (two different estimates used). The line is the best fit to the data. Error bars are smaller than symbol sizes. Notice that only larger lattice sizes were used for this analysis.

model studied does not belong to the three-dimensional Heisenberg universality class. For comparison the critical exponents for the three-dimensional Heisenberg model on a cubic lattice are [27] $\beta = 0.3616(31)$, $\gamma = 1.3896(70)$, and $\nu = 0.7036(23)$.

On the other hand, extending our analysis to lattices as large as $L = 70$, the scenario sensitively changes. As a matter of illustration, we consider here the finite-size scaling analysis of the magnetization at the bicritical point (Fig. 18) for $L = 60$, 64, and 70, from which we obtain an average value of $\beta/\nu = 0.546(4)$, a value far apart from the one obtained for $L \leqslant 40$ [$\beta/\nu = 0.66(1)$] and much closer—albeit not equal—to the expected $\beta/\nu = 0.514(7)$ for the three-dimensional Heisenberg model. In order to obtain the expected exponent ratio, it would be necessary to extend the analysis to even larger lattice sizes, an unnecessary task here, as we could determine the universality class of the model by other means. Finite-size effects may, however, be a serious problem when the universality class of the system studied is not known *a priori*.

[1] W. Selke, Phys. Rev. E **87**, 014101 (2013).
[2] E. C. Andrade, M. Brando, C. Geibel, and M. Vojtal, Phys. Rev. B **90**, 075138 (2014).
[3] R. T. S. Freire, J. A. Plascak, and B. V. Costa, Braz. J. Phys. **34**(2A), 438 (2004).
[4] S.-H. Tsai, S. Hu, and D. P. Landau, J. Phys.: Conf. Ser. **487**, 012005 (2014).
[5] R. T. S. Freire, P. H. L. Martins, and J. A. Plascak, J. Phys.: Conf. Ser. **487**, 012006 (2014).
[6] K. Binder, Z. Phys. B Condensed Matter **43**, 119 (1981).
[7] J. A. Plascak and P. H. L. Martins, Comput. Phys. Commun. **184**, 259 (2013).
[8] P. H. L. Martins and J. A. Plascak, Braz. J. Phys. **34**(2A), 433 (2004).
[9] A. D. Bruce, J. Phys. C: Solid State Phys. **14**, 3667 (1981).
[10] N. B. Wilding and A. D. Bruce, J. Phys.: Condens. Matter **4**, 3087 (1992).
[11] A. D. Bruce and N. B. Wilding, Phys. Rev. Lett. **68**, 193 (1992).
[12] N. B. Wilding, J. Phys.: Condens. Matter **9**, 585 (1997).
[13] J. A. Plascak and D. P. Landau, Phys. Rev. E **67**, 015103(R) (2003).
[14] R. T. S. Freire, S. J. Mitchell, J. A. Plascak, and D. P. Landau, Phys. Rev. E **72**, 056117 (2005).
[15] N. B. Wilding and P. Nielaba, Phys. Rev. E **53**, 926 (1996).
[16] E. Eisenriegler and R. Tomaschitz, Phys. Rev. B **35**, 4876 (1987).
[17] B. Widom, J. Chem. Phys. **43**, 3898 (1965).
[18] L. E. Reichl, in *A Modern Course in Statistical Physics*, 2nd ed. (John Wiley and Sons, New York, 1998).
[19] N. Metropolis, A. W. Rosenbluth, M. N. Rosenbluth, A. H. Teller, and E. Teller, J. Chem. Phys. **21**, 1087 (1953).
[20] U. Wolff, Phys. Rev. Lett. **62**, 361 (1989).
[21] J. A. Plascak, A. M. Ferrenberg, and D. P. Landau, Phys. Rev. E **65**, 066702 (2002).
[22] T. Ala-Nissila, E. Granato, K. Kankaala, J. M. Kosterlitz, and S.-C. Ying, Phys. Rev. B **50**, 12692 (1994).
[23] D. P. Landau and K. Binder, in *A Guide to Monte Carlo Simulations in Statistical Physics* (Cambridge University Press, Cambridge, 2000).
[24] A. M. Ferrenberg, in *Computer Simulation Studies in Condensed Matter Physics III*, edited by D. P. Landau, K. K. Mon and H.-B. Schüttler (Springer-Verlag, Heidelberg, 1991).
[25] A. M. Ferrenberg and R. H. Swendsen, Phys. Rev. Lett. **61**, 2635 (1988).
[26] M. E. J. Newman and G. T. Barkema, in *Monte Carlo Methods in Statistical Physics* (Clarendon, Oxford, 1999).
[27] K. Chen, A. M. Ferrenberg, and D. P. Landau, Phys. Rev. B **48**, 3249 (1993).